Quantification of temperature dependence of NO$_x$ emissions from road traffic in Norway using air quality modelling and monitoring data

Eivind G. Wærsted [a] 👤 ✉ , Ingrid Sundvor [b], Bruce R. Denby [a], Qing Mu [a]

[a] Norwegian Meteorological Institute, Henrik Mohns plass 1, 0313, Oslo, Norway
[b] Norwegian Institute of Transport Economics, Gaustadalléen 21, 0349, Oslo, Norway

Check for updates

Show less ⌃

☰ Outline | ⌁ Share | 🗨 Cite

Highlights

- Road traffic NOx emission increase in cold weather found from dispersion model bias.

- Emissions estimated to be 2.7 (3.3) times higher at -7°C (-13°C) than at >14°C.

- Results agree with literature on emission measurements of individual vehicles.

Abstract

Emissions of nitrogen oxides (NO$_x$) from road traffic are dependent on a range of factors including vehicle type, speed, driving patterns and engine temperature. Recently a number of studies have indicated that ambient air temperature plays an important role in vehicle NO$_x$ emissions, mainly due to various technical challenges of diesel vehicles that occur at low ambient temperatures. This study aims to derive a correction formula to account for this temperature dependence when calculating emissions from road traffic in Norway. Measured NO$_x$ concentrations in the period 2016–2019 at 46 sites dominated by road traffic sources are compared to the NO$_x$ concentrations calculated with the chemistry-transport modelling system EMEP/uEMEP at the same sites. The model has good road traffic volume input data, but no temperature dependence in the emission factors. A clear temperature dependence in the observed-to-modelled ratio of NO$_x$ concentration is found. The ratio increases from 1.09 at high temperatures to 2.9 at low temperatures. The increase occurs gradually in the temperature range from -13°C to +14°C. Assuming this temperature dependence in the bias is due to the road traffic emissions, a correction formula for these emissions is derived. The correction factor is 1 at high temperatures and 3.28 at low temperatures, with a linear increase in the range from +12.4°C to -12.9°C. Thus, our results suggest that road traffic emissions should be 3.3 times higher at temperatures below -13°C than at high temperatures, and 2.7 times higher at -7°C. The temperature range and magnitude of this temperature dependence are consistent with the existing literature on emission measurement experiments performed on various models of diesel vehicles. The derived temperature dependence can be used to correct road traffic emissions. However, the parameter values in the correction are dependent on the vehicle fleet composition and are applicable only for the current Norwegian vehicle fleet.

1. Introduction

Air pollution by <u>nitrogen oxides</u> (NO_x) is an important remaining air quality issue in urban environments in Europe (European Environment Agency, 2020). NO_x consist of the gases <u>nitrogen monoxide</u> (NO) and <u>nitrogen dioxide</u> (NO_2). Both long-term and short-term human exposure to NO_2 are harmful for human health (Huangfu and Atkinson, 2020; Orellano et al., 2020). Especially there is evidence that NO_2 can trigger development or aggravation of asthma and increased susceptibility to respiratory infections (World Health Organization, 2013; Copat et al., 2020; Zheng et al., 2021). While it is NO_2 that is harmful to breathe, concentrations of NO are also relevant as it reacts with ground-level ozone (O_3) to form NO_2.

The most important source of NO_x for human exposure is road traffic (European Environment Agency, 2020), especially diesel vehicles. The NO_x concentration varies strongly in time and space, with local hot-spots in urban areas and near roads. High-resolution modelling is therefore an important complement to the observations at monitoring stations for capturing the spatial variability in order to estimate human exposure. In Norway, the EMEP/uEMEP modelling system is used for such exposure studies, as well as air quality forecasting of NO_2 and other pollutants (Denby et al., 2020). To model NO_2 precisely for these applications, the most important requirement is accurate NO_x emission data at high spatial and temporal resolution. This is challenging as also emission factors per vehicle can vary largely over e.g. type of route and ambient temperature (Söderena et al., 2020).

Pollution levels in urban areas are usually higher on cold winter days due to meteorological conditions; cold weather is often associated with weak winds and little vertical mixing. Any further increase of emissions from vehicles due to low ambient temperatures will hence aggravate the situation. It is therefore important to quantify the temperature dependence, both how much the emissions increase and in which temperature range it occurs.

In this article, the temperature dependence of road traffic emissions is estimated using a "top-down" approach based on observed concentrations, which can be seen as complementary evidence to the more precise "bottom-up" approach of measuring emissions from specific vehicle models directly. By comparing the observed concentrations to those calculated by an atmospheric dispersion model, biases in <u>emission inventories</u> can be analysed. This is a useful approach that is regularly used in air pollution research (e.g. Denby, 2011; Kuik et al., 2018). In our case, the idea is to use observations of NO_x at monitoring stations together with temperature data to find evidence of a temperature dependence of emissions. To separate the effect of emissions from the meteorological effects, we also model the concentrations using a chemistry transport model. The model uses a detailed dataset for road traffic emissions, but without any temperature dependence in the emission factors. From four years (2016–2019) of modelled and observed NO_x concentrations at 46 monitoring stations in Norway, a systematic temperature-dependent bias is found. This is used to derive an empirical correction factor for NO_x emissions as a function of temperature. To our knowledge, this approach for estimating the temperature dependence of NO_x emissions has not been published before.

Deviations between observed and modelled concentrations may be caused by bias in <u>atmospheric transport</u> as well as bias in emissions. To better distinguish these two effects, we also carry out a similar assessment for the concentration of <u>particulate matter</u> (PM) in the size range 2.5–10μm ($PM_{2.5-10}$) as we do for NO_x. Local sources of $PM_{2.5-10}$ are dominated by road traffic non-exhaust particles (road dust) in Norway (see section 4.1.2), and it can therefore be used as an alternative road traffic emission proxy to assess any temperature-dependent bias in model dispersion. We did not include particles smaller than 2.5μm ($PM_{2.5}$) in this analysis because they have a stronger contribution from residential wood combustion than road traffic exhaust in Norway (Grythe et al., 2019).

We start by reviewing the literature on temperature dependence of NO_x road traffic emissions in section 2, and from that we give an estimate of how large an impact temperature can be expected to have on NO_x emissions in Norway. Then, in section 3 we describe the monitoring stations and model setup. In section 4, the temperature-dependent bias in NO_x concentrations we find using our setup is presented, and we argue that a bias in the road traffic emissions is more likely than any other explanation. A correction factor for road traffic emissions is then derived, and we apply it to NO_x calculations for the additional year 2020. Conclusions are given in section 5.

2. Review of experimental evidence

2.1. Reasons for temperature dependence

Type approval emission testing has included low ambient temperature (at about -7°C) for petrol vehicles with the so called Type VI test for about two decades (EU Directive 98/69/EC). The main motivation was risk of high emissions of <u>carbon monoxide</u> (CO) and hydrocarbons (THC) during cold starts. Increasing evidence of higher NO_x emission under real driving conditions for diesel vehicles compared to type approval standards raised concern for the effect of low ambient temperatures also for these vehicle groups (Dardiotos et al., 2012). More evidence was given which further affected the vehicle emission regulation (European Commission, 2021). Even if the change in regulation will lead to overall lower emission and maybe a different temperature dependence for the newest vehicles (Grange et al., 2019), it will take time before this will become noticeable in the fleet. To give an indication of what effect is likely for Norwegian conditions and for the emissions used in the air quality modelling, we here point to findings in the literature.

Low ambient temperatures affect exhaust emissions through several pathways, which vary with fuel type, Euro standard and exhaust aftertreatment system as well as different engine strategies (Suarez-Bertoa et al., 2019; Ko et al., 2017; Weber et al., 2019). Temperature effects can be due to, for instance, increased air resistance, higher engine friction, the need for heating the cabin, more severe cold-start conditions and sub-optimal functioning of exhaust aftertreatment systems. Especially the last two affect the NO_x emissions for diesel vehicles (Suarez-Bertoa et al., 2019; Ko et al., 2017; Weber et al., 2019). For NO_x reduction in diesel vehicle exhaust the main technologies applied are <u>Exhaust Gas Recirculation</u> (EGR), Selective Catalytic Reduction (SCR) and Lean NO_x Trap (LNT). Even if temperature also affects the NO_x emissions of petrol vehicles, the overall level is still low (Dardiotos et al., 2013; Grange et al., 2019; Tu et al., 2021) compared to diesel vehicles. The contribution from petrol vehicles is estimated to make up about 6% of the total road traffic emissions (see Table 1). Therefore, we here limit the focus to the effect on diesel vehicles. Temperature also affects other emissions, e.g. particle emissions (Wang et al., 2018), but that is outside the scope of this article, and moreover road traffic exhaust is a minor source of particle pollution during winter in Norway.

Table 1. Emission factors (EFs) and percentage of kilometres driven in the Norwegian fleet for different vehicles in year 2018: Heavy duty vehicle (HDV), light commercial vehicle (LCV), passenger car (PC) and bus. The last column gives the contributions to total road traffic NO_x emissions, by combination of the two first columns.

Vehicle type	Fuel	EF NO_x [g/km]	% of km	% of emissions
HDV	diesel	2.36	4.43	18.4
LCV	diesel	0.57	15.52	15.6
LCV	petrol	0.52	0.45	0.4
LCV	electricity	0.00	0.10	0.0
PC	diesel	0.62	43.85	47.9
PC	petrol	0.12	23.34	4.9
PC	electricity	0.00	5.24	0.0
PC	hybrid-diesel	0.31	0.27	0.1
PC	hybrid-petrol	0.11	5.65	1.1
Bus	diesel	5.82	1.13	11.6
Bus	electricity	0.00	0.02	0.0

Inquiries after the "diesel scandal" revealed that manufacturers actively limited the effect of the NO_x exhaust aftertreatment systems with the argument of condensation on the EGR and risk of soot build up. One manufacturer reported start of deactivation already at 17°C (European Union, 2016) while it was observed for another manufacturer at 12°C (Bernard et al., 2019). Hence, it is likely that such a temperature effect is present for a large part of the year in most regions in Norway. The strategies are not equal for all manufacturers, but they all operate with a "thermal window". In that case, each diesel vehicle will at some lower temperature have a non-functioning control strategy or deactivated exhaust aftertreatment system targeting NO_x. Therefore, a steady increase of emissions from the fleet with decreasing temperatures can be expected until a cut off-temperature where no further effect will occur.

With larger temperature differences to the ambient air the engine will cool off faster and have increased heat-up times. This will lead to more cold starts as well as longer time of a trip in cold-start mode (Weber et al., 2019). Especially for passenger cars (PCs) this is relevant, since they have more short trips (Faria et al., 2018) compared to heavy duty vehicles (HDVs) and buses which operate more continuously (Hovi et al., 2019; Thorne et al., 2021). Faria et al. (2018) found that at 0°C PCs in urban driving spent about 80% of the time in cold phase.

2.2. Quantitative studies

Several studies have performed emission measurements on diesel vehicles, especially PCs, under different conditions including low ambient temperatures, both with cold- and hot-start, and using different measurement setups like portable emission measurement systems (PEMS) on road, <u>dynamometer</u> with different test driving cycles or <u>remote sensing methods</u>. Weilenmann et al. (2009) tested six Euro-4 PCs on a dynamometer with an urban driving cycle, and found on average 4g/start extra NO_x at -20°C compared to 23°C, which can be a significant increase when compared with basic emission factors. If we compare this with the emission factor applied in our modelling for diesel PC (Table 1), it would be equivalent to more than 6km of driving. Dardiotos et al. (2013) tested one Euro 4, three Euro 5 and one Euro 6 compliant vehicles over the New European Driving Cycle (NEDC). NO_x emissions increased for all vehicles at -7°C compared to 20°C with one vehicle showing close to 9 times more during one part of the driving cycle, but the average for all vehicles tested was between 4 and 5 times more. Lapuerta et al. (2018) found an increase of about 8 times for one Euro 6 vehicle also using the NEDC while Weber et al. (2019) using NEDC, Artemis Urban and a Helsinki city cycle found an increase of approximately 3 times at -7°C, which is also similar to the results from Suarez-Bertoa and Astorga (2018) with an average of a 3.4 times increase for five vehicles tested with the World harmonised Light-duty Test Cycle (WLTC). Grange et al. (2019) used a <u>remote sensing</u> on-road setup and found different increases for different Euro 6 types depending on the exhaust aftertreatment system, but with a relative increase of 1.6–2 at 0°C on average. Pre-Euro 6 was found to have higher emissions overall, but a rather similar relative increase of 1.67 at 0°C. The Handbook Emission Factors for Road Transport (HBEFA) has included a linear increase of NO_x emission factors for diesel cars with decreasing temperature, with about a doubling of emissions for Euro 6 at 0°C, but no further effect for lower temperatures (Hausberger and Matzer, 2017).

There is overall less literature on the evidence of increased NO_x emissions for HDVs at low ambient temperatures, but Grigoratos et al. (2019) tested four Euro VI trucks and one bus on-road with PEMS and for different speed conditions. They conclude that the emissions from Euro VI are considerably lower than previous Euro classes, but that NO_x emissions increase for conditions when air/fuel ratio is not optimal (urban driving) and/or when the Selective Catalytic Reduction (SCR) does not reach high enough temperatures. This is also given as an explanation for why one vehicle, tested in cooler temperatures (7–11°C), had 5-11 times higher emissions than the best performing vehicle at low and high speed conditions respectively. This is further supported by other studies which show that NO_x emissions are strongly dependent on the SCR temperature (McCaffery et al., 2021). Söderena et al. (2021) monitored Euro VI buses in real operation with continuous measurements, as well as chassis dynamometer and on-road PEMS testing. They found a 2–4 times increase of NO_x for below zero temperatures in winter periods compared to summer conditions. If the challenge with low temperatures and NO_x emissions mainly is related to non-functional exhaust aftertreatment systems (i.e. SCR, EGR and LNT) then an indication of the effect can also be given by studies looking into tampering, where the exhaust aftertreatment systems are actively being reduced or deactivated (or removed/damaged). This has been reported to give a massive increase in emissions if the engine-out NO_x emissions were to be directly emitted, and would put Euro V and Euro VI back to Euro II-Euro I levels. This means an increase of up to 4 or 12 times (Hooftman and de Ruiter, 2019).

The experimental studies use different measurement setups and the emission factors found are often test cycle/method dependent. This makes it challenging to compare results with regard to separating the different effects from each other (e.g. extra cold start contribution in low ambient temperature vs. other effects). However, there is clear evidence for a significant increase of NO_x emissions from diesel vehicles with decreasing temperatures. Nevertheless, the effect on the overall emissions from the vehicle fleet over time and space is still challenging to quantify precisely and many relevant factors are still unknown (e.g. number or fraction of cold starts) and also too vehicle dependent (i.e. dependent on engine strategies (Weber et al., 2019). There are also few studies including temperatures below -7°C.

2.3. Estimated temperature effect for the vehicle fleet

To get an indication of what effect temperature will have on the overall road traffic emissions, we perform a small, simplified calculation. An overview of the emission factors (EF) and the percent of kilometres driven for each vehicle and fuel type, used as the basis for the emission input data in the model, is given in Table 1 (see also section 3.3). From the table one can deduce that diesel vehicles – adding up HDVs, buses, light commercial vehicles (LCVs) and PCs – dominate the NO_x emissions, accounting for 94% of the total. No Euro class specification is given in Table 1, but from vehicle age statistics by Statistics Norway (SSB) we have estimated that the fraction of kilometres driven with diesel vehicles that are Euro-4/IV or newer is 92% for PCs, 93% for LCVs, and 97% for HDVs and buses. Using the Euro class specific emission factors derived in Matzer et al. (2019), we estimate that 82% of the road traffic NO_x emissions come from diesel vehicles of Euro 4/IV or newer. Based on sections 2.1 Reasons for temperature dependence, 2.2 Quantitative studies the temperature dependence is expected to be most prominent for these vehicles.

Even if there are some findings of more than 8 times more emission for single vehicles in specific driving conditions at low temperatures, averages from studies with more vehicles and also using different experimental setups are in the range of a 2–4 times increase at sub-zero temperatures. Since the diesel vehicles of Euro 4/IV and newer are dominating the total NO_x road traffic emissions, this is also the range we then could expect of the temperature correction needed. This is given as a relative effect compared to emissions at rather warm temperatures (typically around 23°C). To see a similar effect in the modelled data, an assumption will then also have to be that the emissions used at this temperature (see Table 1) are comparable with emissions of vehicle models included in the experimental studies. It is expected that Euro 6 has a different relative increase than Euro 4, but we here do not differentiate on Euro classes.

3. Methodology

3.1. Monitoring stations

We use observations from the network of <u>air quality monitoring</u> stations in Norway. Most of these measurement sites have been established to comply with European and Norwegian legislation for air quality monitoring of each air quality zone (EU Directive 2008/50EC). We have obtained the observed concentrations from these stations through a public API (https://api.nilu.no↗). Monitoring data have been quality controlled and aggregated to hourly mean concentrations by the Norwegian National Air Quality Reference Laboratory, which is currently the Norwegian Institute for Air Research (nilu.no), following the procedures detailed in the guidance document (Norwegian Environment Agency, 2014).

We have included stations classified as traffic or urban background that measured either NO_x or $PM_{2.5-10}$ concentrations during the period 2016–2019. There are 52 such stations. However, two of the urban background stations have been excluded because the model (see section 3.2) found that shipping or industry emissions were as important as road traffic exhaust at these sites. There are also two industrial stations and a regional background station that measure NO_x, but these are excluded. Table 2 presents the number of stations that measure each component. $PM_{2.5-10}$ is calculated from observations of PM_{10} and $PM_{2.5}$.

Table 2. The number of stations of each type included in this study that measure NO_x, $PM_{2.5-10}$ (i.e. PM_{10} and $PM_{2.5}$) and both.

Station type	NO_x	$PM_{2.5-10}$	Both
Traffic	39	37	35
Urban background	7	8	6

As can be seen from Table 2, most of the stations that measure NO_x also measure PM_{10} and $PM_{2.5}$, and vice versa. About two thirds of the stations cover at least 75% of the 4-year period, and only two stations cover less than 25%. Most of the stations are either in or close to the cities and larger towns, and more than half of them are in Greater Oslo or in towns in southeastern Norway. The majority of stations are traffic stations, while urban background concentrations are only measured in a few cities. Table 3 shows some more details about each traffic station that measures NO_x. The mean NO_x concentration varies from over $100 \mu g/m^3$ at three stations in Greater Oslo to only $14.1 \mu g/m^3$ at one station. The traffic amount and share of heavy vehicles[1] on the road also varies importantly between the traffic stations.

Table 3. The 39 traffic stations measuring NO_x: After station name and location, the columns are the Annual Daily Traffic (ADT) and the percent of long vehicles (see section 3.3.1) at the road link with highest ADT within 100m, the winter mean temperature (all hours in January, February and December 2016–2019) from Met Nordic analysis (see section 3.4), the 4-year mean observed NO_x concentration (all months), and the percentage of the 4-year period covered with NO_x observations.

EOI	Station name	Latitude°N	Longitude°E	Region	ADT	long%	T_{DJF}°C	$[NO_x]\mu g/m^3$	cov%
NO0057A	Alnabru	59.927 7	10.846 6	Greater Oslo	26 028	10	−1.4	116.5	95
NO0093A	Hjortnes	59.911 3	10.704 0	Greater Oslo	76 991	12	−0.3	105.7	99
NO0122A	E6 Alna senter	59.925 6	10.850 4	Greater Oslo	97 950	12	−1.5	102.3	51
NO0095A	Smestad	59.932 5	10.669 9	Greater Oslo	51 292	6	−1.1	97.3	98
NO0083A	Bygdøy Alle	59.919 3	10.696 5	Greater Oslo	19 953	9	−0.5	94.5	91
NO0071A	Manglerud	59.898 7	10.814 9	Greater Oslo	74 463	11	−1.7	93.5	99
NO0129A	Solheim	59.928 6	10.953 2	Greater Oslo	51 210	6	−2.5	89.6	50
NO0099A	Eilif Dues vei	59.906 1	10.612 0	Greater Oslo	88 060	8	−1.1	70.9	99
NO0067A	Bangeløkka	59.733 3	10.211 7	Greater Oslo	23 100	10	−1.8	69.2	95
	Åkebergveien	59.912 0	10.767 4	Greater Oslo	7329	6	−0.4	62.2	78
NO0011A	Kirkeveien	59.932 3	10.724 5	Greater Oslo	20 099	13	−1.5	57.5	93
NO0112A	Kransen	59.433 5	10.661 8	Greater Oslo	19 216	11	−0.4	50.2	43
NO0101A	Rv 4, Aker sykehus	59.941 0	10.798 0	Greater Oslo	47 711	8	−1.5	47.3	97
NO0114A	Bekkestua	59.918 2	10.583 9	Greater Oslo	9460	7	−1.6	45.1	72
NO0111A	Vigernes	59.955 5	11.074 0	Greater Oslo	18 286	10	−2.6	40.8	96

EOI	Station name	Latitude°N	Longitude°E	Region	ADT	long%	T_{DJF}°C	[NO_x]µg/m³	cov%
NO0084A	St.Croix	59.210 3	10.945 4	Southeast Norway	27 096	8	0.0	77.7	87
	Hønefoss skole	60.170 9	10.261 6	Southeast Norway	17 700	10	−3.4	63.1	25
NO0074A	Bankplassen	61.113 0	10.464 9	Southeast Norway	17 800	6	−5.2	62.3	92
NO0103A	Minnesundvegen, Gjøvik	60.790 9	10.696 7	Southeast Norway	15 523	7	−4.0	58.3	93
NO0104A	Vangsveien, Hamar	60.796 5	11.097 8	Southeast Norway	16 100	8	−4.2	49.9	50
NO0110A	Alvim	59.273 8	11.089 2	Southeast Norway	16 657	7	−0.4	47.3	55
NO0061A	Lensmannsdalen	59.159 3	9.635 7	Southeast Norway	16 200	9	−1.0	45.2	98
NO0130A	Ringsakervegen	60.885 9	10.937 8	Southeast Norway	10 300	8	−4.5	39.8	38
NO0119A	Leiret	60.883 6	11.559 3	Southeast Norway	19 200	10	−5.7	39.4	69
NO0128A	Nedre Langgate	59.263 7	10.411 2	Southeast Norway	16 400	8	−0.4	38.3	4
NO0106A	Sverresgate	59.138 1	9.652 1	Southeast Norway	5868	5	−0.8	36.1	97
NO0092A	Gartnerløkka	58.146 9	7.986 6	South Norway	28 500	9	2.1	62.5	95
NO0059A	Danmarks plass	60.374 1	5.340 2	West Norway	48 400	9	3.3	88.2	99
NO0109A	Loddefjord	60.361 1	5.236 9	West Norway	22 500	6	2.7	87.3	98
NO0121A	Rådal	60.294 3	5.324 6	West Norway	40 000	9	2.6	71.1	57
NO0076A	Kannik	58.964 1	5.727 9	West Norway	34 000	8	3.3	68.3	69
NO0125A	Schancheholen	58.951 9	5.721 9	West Norway	28 600	7	3.3	51.0	35
NO0116A	Karl Eriksens plass	62.470 6	6.153 5	West Norway	15 200	7	3.6	49.1	69
NO0060A	Elgeseter	63.419 2	10.395 9	Trondheim	20 980	12	−0.4	79.6	88
NO0102A	E6-Tiller	63.357 6	10.371 7	Trondheim	27 100	15	−1.3	64.1	86
NO0068A	Bakke kirke	63.433 0	10.410 9	Trondheim	12 700	0	−0.1	46.0	88
NO0079A	Hansjordnesbukta	69.656 2	18.963 7	North Norway	17 250	5	−2.6	75.7	89
NO0127A	Seljestad Rv83	68.792 2	16.537 4	North Norway	18 000	4	−1.6	60.0	46
NO0126A	Olav V gate	67.275 5	14.419 1	North Norway	11 956	8	−0.3	14.1	27

3.2. Model setup

NO_x, $PM_{2.5}$ and PM_{10} concentrations are modelled for each hour at the location of each monitoring station using the EMEP/uEMEP modelling system. The model setup is similar to the one used in the Norwegian operational air quality forecasts, which is described in section 4 of Denby et al. (2020). In short, the concept is to use Gaussian plume modelling (uEMEP model) for nearby emission sources (within 10km x 10km), and use gridded concentrations from the EMEP MSC-W chemistry transport model (EMEP model) (Simpson et al., 2012) for sources further away. In this way, the model system can capture fine-scale hot-spots in concentrations around emission sources such as roads, and at the same time model all of Norway using acceptable computational resources.

These are the steps of the calculation:

1. The EMEP model is run for Europe at 0.1° resolution, using meteorology from the Integrated Forecasting System from the European Centre for Medium-Range Weather Forecasts (ECMWF, 2020) and the CAMS-REG-AP_v1.1 regional anthropogenic emission dataset (Kuenen et al., 2014; Granier et al., 2019).

2. The EMEP model is run for a smaller domain covering Norway and parts of the surrounding Nordic countries at 2.5km resolution, using the first run as boundary conditions. This run uses meteorology from the first 24h of the operational weather forecast with the AROME-MetCoOp model (Müller et al., 2017) that is initialized at 00 UTC every day. Inside of Norway it uses more detailed national emissions for four GNFR[2] sectors (see section 3.3), while the CAMS-REG-AP_v1.1 emissions are used for all other sources.

3. uEMEP is used to model the contributions from these four GNFR sectors at each station from sources within a 10km x 10km area at a higher spatial resolution, using Gaussian plume modelling (250m for sectors B, C and G, and 25m for F). Details are given in Denby et al.

(2020).

4. The non-local contribution is calculated by subtracting the contributions that the downscaled sources have in the EMEP model from the EMEP grid concentration, thus avoiding double counting (Denby et al., 2020).

3.3. Emissions

National emission datasets with higher spatial resolution and precision than CAMS-REG-AP_v1.1 have been developed for Norway for four GNFR sectors: industry (B), residential combustion (C), road traffic (F) and shipping (G). Road traffic is the most important of these sectors, both for NO_x and $PM_{2.5-10}$, and is the main focus of this article. The emission data for this sector are therefore described briefly. Further details about emissions from all four sectors are presented in the supplementary material of Denby et al. (2020).

3.3.1. Road traffic volume

Average road traffic volume of long (>5.6m) and short (<5.6m) vehicles on all roads in Norway are available from the national road database (NVDB, 2020), based on a network of more than 2000 stations continuously measuring traffic volume (https://trafikkdata.no↗) and a traffic model (Nordbeck and Langsrud, 2015). The traffic is distributed in time using an empiric weekly cycle of traffic with 168 hourly factors, which is different for long and short vehicles.

3.3.2. Road traffic exhaust emissions

Total exhaust emissions of NO_x and other pollutants from road traffic in Norway for each year are calculated by SSB (Holmengen and Fedoryshyn, 2015). They use the traffic volume together with emission factors calculated using the HBEFA emission model (Hausberger et al., 2009) applied to the distribution of fuel technologies being used in the Norwegian vehicle fleet.

We use the SSB emission total for 2018 and distribute it in space using the traffic volume dataset, weighing long vehicles five times more than short vehicles and assuming all HDVs and buses and 25% of LCVs are long vehicles. This setup means that, for long and for short vehicles, the same average emission factor is used everywhere; thus we do not take into account that the vehicle age and fuel technology varies between the Norwegian municipalities (e.g. a larger share of electric vehicles in the big cities). When applying the emissions to the other years, the trend in total NO_x emissions of -7.5% per year in the period 2016–2019 found by SSB (Statistics Norway, 2020) has been adjusted for in uEMEP.

3.3.3. Road traffic non-exhaust emissions

Non-exhaust particles generated by road, tyre and brake wear contribute significantly to the $PM_{2.5-10}$ concentrations in Norway, especially in the winter season when studded tyres are used (Denby et al., 2018). The emissions of non-exhaust particles depend strongly on the road moisture conditions. The generation, build-up and emission of the non-exhaust particles on all road links in Norway are modelled by the NORTRIP road dust model (Denby et al., 2013a,b). Due to the sensitivity to road moisture conditions, which are also modelled, the non-exhaust emissions are more uncertain and more variable than exhaust emissions on shorter times scales. However, for long term statistics over many stations the results for non-exhaust modelling show quite good results (Denby et al., 2020).

3.4. Temperature data

Temperature is not measured at most of the NO_x monitoring stations. To get the best estimate for temperature for each hour at each station, we have linearly interpolated from the gridded temperature analysis dataset of the Norwegian Meteorological institute at 1 km resolution (Met Nordic analysis). This dataset uses statistical methods to combine the 6-h weather forecast temperatures at 2.5 km resolution with station observations, making use of spatial proxies such as topography and meteorological features in the forecast ensemble to interpolate the temperature corrections in space in a realistic way (Lussana et al., 2019; Nipen et al., 2020). This temperature is used for studying the temperature dependence of NO_x concentrations both in the model and in observations. Since most of the road traffic emissions come from roads near the station, the temperature at the station should be a good estimate of the ambient temperature where these emissions occur.

3.5. Data sampling

Analysed temperature and modelled concentrations are available for all hours at all the stations. The observed concentrations are not always available, either because the quality control has removed the observations or because the measurements were not operating at the station for the whole 4-year period. When we calculate the averages that are shown in section 4, we include only the hours when the observed concentration is available. However, NO_x and $PM_{2.5-10}$ results are sampled separately: in the results for NO_x, we include all the hours with the NO_x observation from a station regardless of whether or not the $PM_{2.5-10}$ observation is available at the same time, and vice versa.

4. Results and discussion

4.1. Overview of model vs. observations

4.1.1. NO_x

Fig. 1a and b compares modelled and observed concentrations of NO_x over the four years. Fig. 1b shows that the model underestimates NO_x concentrations significantly at most stations, in particular at the traffic stations. Fig. 1a shows that the bias has a clear seasonal cycle. The NO_x concentrations are higher in winter than in summer both in the model and in observations, but the magnitude of this seasonal cycle is much stronger in the observations. In summer there is only a weak negative bias, while this bias is about a factor two in winter. The annual cycle of station-mean temperature is also shown. In section 4.2 we will analyse in more detail how temperature can explain the seasonal cycle in bias.
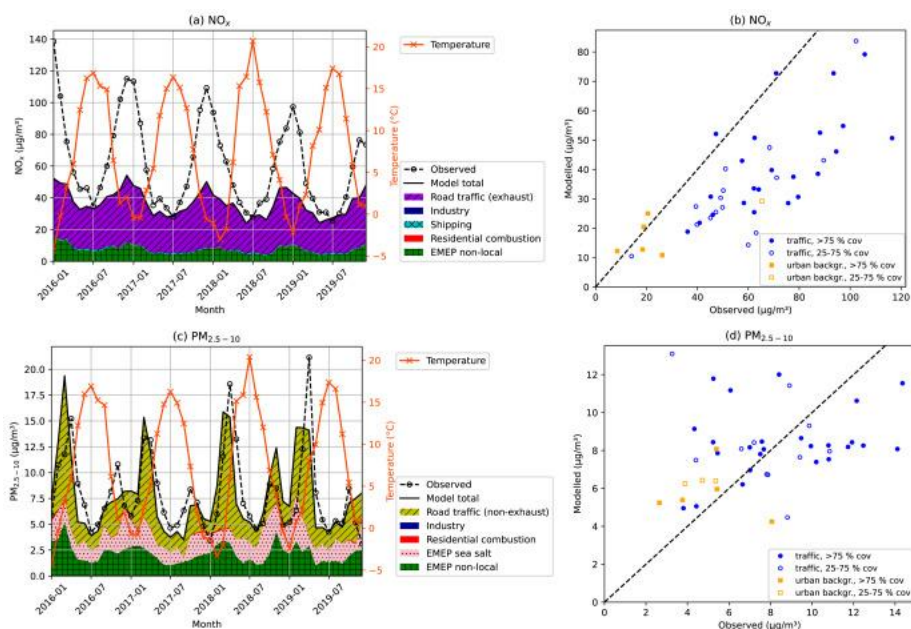
Download : Download high-res image (1MB)

Download : Download full-size image

Fig. 1. Statistics of observed and modelled concentrations in the period 2016–2019: Subplot a/c shows the monthly time series of observed NO_x/$PM_{2.5-10}$ concentration, and the modelled concentration, which is divided into sector contributions, and temperature from Met Nordic analysis. Data have been aggregated by averaging over all stations with available observations at each hour, and then taking the monthly mean. Subplot b/d shows the NO_x/$PM_{2.5-10}$ concentration averaged over the 4-year period at each station, plotting modelled vs. observed concentration, and indicating the type of station. Stations with data coverage of at least 75% are shown as filled symbols, stations with between 25% and 75% data coverage are unfilled, and stations with less than 25% coverage are not shown.

Fig. 1a also shows how much of the NO_x comes from each emission sector. This sectoral information is only saved for "local" emissions that are recalculated with the Gaussian model (i.e. for emissions within a 10km x 10km area surrounding the station, see section 3.2). The majority of the modelled NO_x concentration is emitted from local road traffic exhaust (78%). Local industry, shipping and residential combustion contribute very little, which is not surprising since stations where shipping and industry are important have been excluded from the study. The final category "EMEP non-local" is the second-most important contribution to NO_x (19%) and comprises all the contributions that are not recalculated with the Gaussian model. This includes the road traffic, shipping, residential combustion, and industry emissions from outside the 10km x 10km domain as well as all other sectors. From a simulation where we studied contributions from abroad, we know that sources outside Norway only contribute about $1 \mu g/m^3$ to NO_x on average (about 15% of the non-local). A run for 2020 that we performed with a larger and more detailed source tracking area indicates that road traffic, shipping, industry and off-road machinery all give contributions of similar importance to the non-local contribution from within Norway.

4.1.2. $PM_{2.5-10}$

Fig. 1c and d shows the same statistics as in a-b but for the $PM_{2.5-10}$ concentration. As explained in section 1, $PM_{2.5-10}$ is not the main focus of this paper, but it is used as an independent road traffic emission proxy for distinguishing emissions and atmospheric transport as explanations for the bias in NO_x. Fig. 1c shows that $PM_{2.5-10}$ contributions are mostly from local non-exhaust road traffic emissions (47%), EMEP non-local (27%), and EMEP sea salt (25%). The EMEP sea salt sector is a natural source of PM which is not downscaled, but it can be shown separately from the rest of EMEP non-local because the speciation of PM is tracked in the EMEP model. The $PM_{2.5-10}$ concentration has a notable seasonal cycle, but compared to NO_x the maximum occurs in late winter and spring instead of mid-winter. The seasonal cycle is well captured by the model and is due to non-exhaust road dust that is generated by road, tyre and brake wear (see section 3.3.3). These dust particles build up on

roads predominantly during winter due to studded tyre usage and are resuspended into the atmosphere especially in the end of the winter season when roads dry up (Denby et al., 2018).

The 4-year mean of $PM_{2.5-10}$ concentration varies much less from station to station than the NO_x concentration (Fig. 1d vs. b). However, the traffic stations have systematically higher concentrations than the urban background stations, which is explained by road dust episodes.

4.2. Assessment of temperature dependence

Fig. 2a shows the NO_x concentration plotted against temperature in the model and observations, averaged over all data at all the stations over the four years. There is a clear temperature dependence in the observations in the range from about -10°C to +10°C. The modelled concentrations also have a temperature dependence in this range, but it is much weaker.
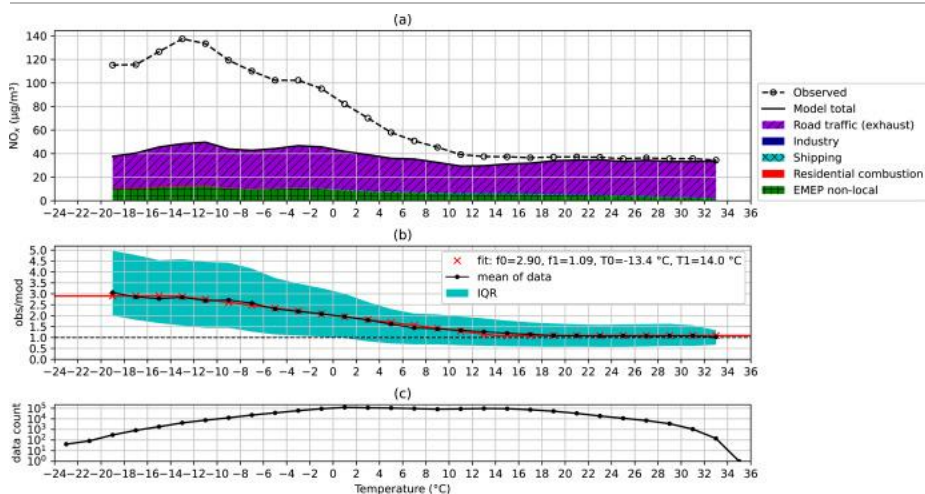
Download : Download high-res image (840KB)

Download : Download full-size image

Fig. 2. Statistics of observed and modelled NO_x concentration vs. analysis temperature in 2016–2019 at 46 monitoring stations: (a) For each 2°C temperature interval ([-20, -18], [-18, -16], etc.), all data with analysis temperature within that range have been averaged, weighing each hour with data at each station equally. The average observed NO_x concentration is shown as a circle for each temperature bin. The mean modelled NO_x concentration in each bin is indicated with the solid line, under which the shaded areas indicate the sectoral contributions. (b) For each temperature bin, the black dot shows the ratio of the observed and modelled mean NO_x concentrations. The line with crosses indicates the linear fit $f(T)$ (Equation (1)). The shaded area indicates the interquartile range (IQR) of observed-to-modelled ratio of single hourly data values in each bin. (c) The number of hourly data values contained in each temperature bin. Only bins with at least 100 data values are plotted in (a) and (b).

The ratio of observed mean to modelled mean concentration for data within each temperature bin is plotted in Fig. 2b. Above ca. 15°C this ratio is close to 1 and constant with temperature. Below 15°C the ratio increases close to linearly with decreasing temperature until ca. -14°C, below which the increase is much weaker. At the lowest temperatures the ratio is close to 3. An indication of the variability of the observed-to-modelled concentration ratio in the dataset within each temperature bin is also shown in Fig. 2b. It confirms the gradual increase when temperatures decrease that is seen in the mean concentration ratio, although the levelling-off at low temperature is not as clear.

The large deviation between modelled and observed NO_x concentrations at lower temperatures can be the result of a number of factors. These are further discussed in section 4.4, but for the time being we consider this deviation to be chiefly the result of increased road traffic emissions of NO_x at low temperatures.

The temperature dependence of observed-to-modelled NO_x ratio corresponds well with causes explained in section 2, especially the effect of more and more vehicles having reduced efficiency of the exhaust aftertreatment system and driving more in cold-phase. The levelling-off at high temperature is interpreted to happen because the exhaust aftertreatment systems function well for all vehicles when it is sufficiently warm, and the levelling-off at low temperature because below a certain temperature all the vehicles will have reached the most sub-optimal situation.

We applied curve-fitting to find the best fit to the mean of data in Fig. 2b, using a function of temperature $f(T)$ that changes linearly between two constant values f_0 and f_1 in a particular temperature interval $[T_0, T_1]$:

$$f(T) = \begin{cases} f_0 & \text{if } T \leq T_0 \\ f_0 + \frac{f_1 - f_0}{T_1 - T_0}(T - T_0) & \text{if } T_0 < T < T_1 \\ f_1 & \text{if } T \geq T_1 \end{cases} \tag{1}$$

The curve-fitting resulted in these coefficient values: $f_0 = 2.90$, $f_1 = 1.09$, $T_0 = -13.4\,°C$, and $T_1 = 14.0\,°C$. This fit is plotted in Fig. 2b. It indicates that the observed NO_x concentration is 9% higher than in the model at high temperatures and 2.9 times higher at the lowest temperatures.

4.3. Variations in temperature dependence

4.3.1. Inter-annual and seasonal variability

Fig. 3 shows the temperature dependence in observations and model for each of the years separately. To avoid sampling bias when comparing different years, only stations that have at least 75% data coverage in all years have been included. Differences in observed concentrations at low temperatures are significant between the years (Fig. 3a). These differences are to some extent captured by the model, so that the observed-to-model fraction (Fig. 3b) is less different between the years than the observations. The observed-to-modelled fraction has a similar temperature dependence in all the years, indicating that the temperature-dependent bias occurs every year. However, in 2016 the overall bias is still stronger than the other years, and most of the bias at high temperature comes from this year.
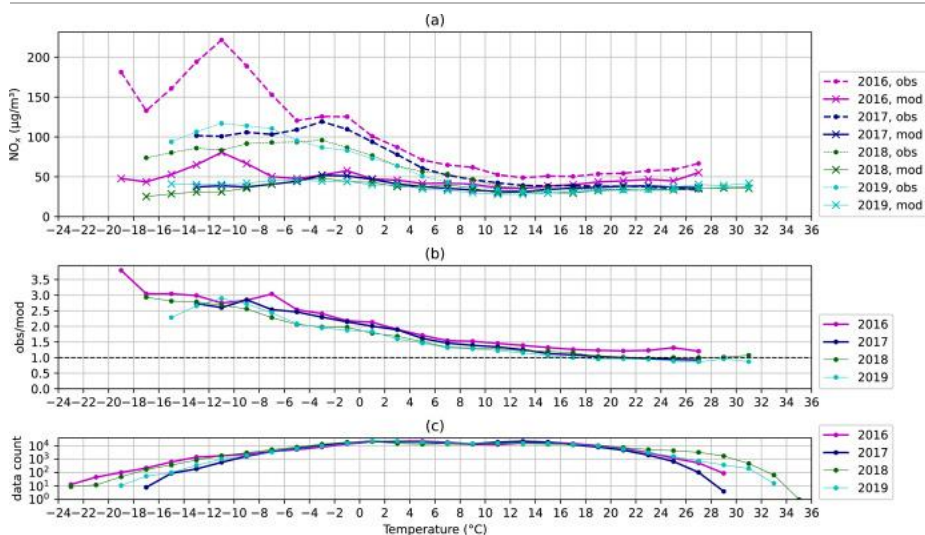
Download : Download high-res image (860KB)

Download : Download full-size image

Fig. 3. Same as in Fig. 2, but shown separately for each year, and without showing sectoral contributions in the model. Only data for stations with at least 75% data coverage in all four years are included. This is 26 stations out of 46.

Fig. 4 shows that the temperature dependence in observed-to-modelled NO_x ratio occurs also when considering each season separately, and the increase with decreasing temperature starts at roughly +14 °C in all seasons. This indicates that the temperature dependence is really related to the temperature, and not just a seasonal cycle caused by something else.
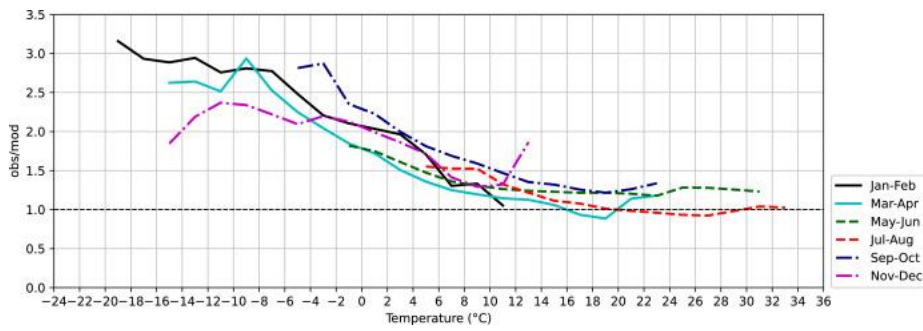
Fig. 4. Same as Fig. 2b, but showing the data separately for six different periods of the year, each covering two months. Only temperature intervals with at least 100 data values in the period are shown.

4.3.2. Spatial variability

We also plotted Fig. 2a separately for each station (not shown) and found that nearly all stations have an increase of observed NO_x concentration with decreasing temperature which is stronger than that of the modelled concentration. However, its magnitude and the temperature range in which it occurs are not exactly the same for each station. Fig. 5 summarises the temperature dependence at each station by plotting the observed-to-modelled NO_x ratio for temperatures between -10 and -4°C normalised by the ratio for temperatures above 14°C, for each station. The interval from -10 to -4°C was chosen because many stations have very few occurrences of temperature below -10°C. In this interval the observed-to-modelled ratio of NO_x is on average 2.2 times larger than at the high temperatures according to the fit in Fig. 2.
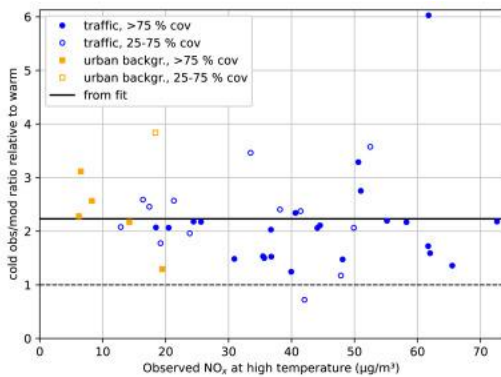
Fig. 5. Temperature dependence at each station: Each dot represents a station. The x-axis is the mean observed NO_x concentration at temperatures >14°C. The y-axis is the ratio of observed to modelled mean NO_x concentration for data with temperatures in the range -10 to -4°C, normalised with the same ratio for data with temperatures >14°C. The y-axis is an indication of how much higher the observed-to-modelled ratio of NO_x is at low temperatures than at high temperatures. Marker symbols have the same meaning as in Fig. 1b/d. Stations with less than 100 data values in one of the two temperature intervals are also excluded. The solid line indicates the expected y-value based on the fit found in Fig. 2b (i.e. $f(-6.2°C)/f_1$, because -6.2°C is the average temperature of the data in the range -10 to -4°C).

Most of the stations are quite close to this average value, but some stations deviate. The station which has 6 times higher ratio at low temperature is in Bergen, which has rather mild winters. Most of the hours with temperature below -4°C at this station occurred during a few episodes in the winter, and it is suspected that the model did not sufficiently capture inversion situations that led to the high concentrations. At the opposite extreme, some stations have almost no change in the ratio between the two temperature intervals (dots close to y=1).

The variation in temperature dependence between stations could be caused by variation in the vehicle fleet composition compared to the one used in the emission calculation. However, over- and underestimation of NO_x concentrations in single episodes could also occur due to bias in wind direction or in meteorological variables affecting dilution (as mentioned for the Bergen station above). We therefore cannot expect the temperature dependence to be as clear in the smaller data sample that a single station represents as in the full dataset including all stations.

We switched the x-axis in Fig. 5 to see if ADT, long vehicle percentage or winter mean temperature (columns in Table 3) could explain some of the spatial variability in the temperature dependence (not shown). However, no relationship was found for these variables. The distribution of fuel technologies and vehicle ages might have been able to explain more, if these data were available at each station.

Traffic and urban background stations are shown separately in Fig. 5. Although the concentrations are lower in general at the urban background stations, we see that they have a similar temperature-dependent relative bias as the traffic stations.

4.4. Alternative explanations

We have found a temperature-dependent bias in the model that is rather consistent in time and space. We assume that the bias is not due to problems with the observations in cold conditions. Thus, the bias must be due to a temperature-dependent underestimation of NO_x concentrations in the model at the measurement stations. However, a temperature-dependent emission factor from road traffic is not the only possible explanation. In this section we will consider two alternative explanations for the temperature dependence:
1. The NO_x emissions are underestimated at low temperatures for a different reason.

2. The model systematically overestimates dilution at low temperature.

Regarding point 1, we will first consider the possibility that NO_x emission underestimation occurs in a different sector than road traffic. If this were true, then we would expect the exposure to this sector to be similar for traffic and urban background stations, so that the absolute increase in observed-to-modelled ratio in NO_x concentration from high to low temperature should be the same for the two station types. Since absolute concentrations are much higher for the traffic stations, then the relative increase should be much smaller for the traffic stations. However, Fig. 5 shows that the relative increase is similar for the two station types, which is consistent with the underestimation being in the road traffic sector. If the road traffic emissions are underestimated in cold conditions, then either the traffic volume or the emission factors are underestimated. Since it is unlikely that the traffic volume is much higher at cold days than warm days, it must be the emission factors.

Regarding point 2, dilution of pollutants can be reduced on cold days because low temperatures often occur as a result of high-pressure situations in the winter when clear skies and little wind lead to a stable boundary layer that inhibits turbulent mixing. In areas where pollution is emitted near the surface, both low wind speed and little vertical mixing will limit dilution and lead to elevated concentrations. Gryning et al. (1987) pointed out the difficulties in Gaussian plume modelling under stable conditions and this remains a problem for these types of models.

In Fig. 6, we have categorised the dataset into periods with stable, neutral and unstable conditions, using the modelled Obukhov length. Assuming that the stability regime is correctly modelled, we see that for temperatures below 6°C, the underestimation of NO_x by the model is slightly larger in stable conditions than in neutral or unstable conditions. The occurrence of stable conditions also rises with decreasing temperature. This might indicate that some of the temperature-dependent bias stems from too much vertical mixing in stable conditions; however, it could also be that the model overestimates the vertical mixing in unstable conditions. It should also be noted that below -10°C, the underestimation of the NO_x concentration is as strong in the unstable and neutral regimes as in the stable regime.
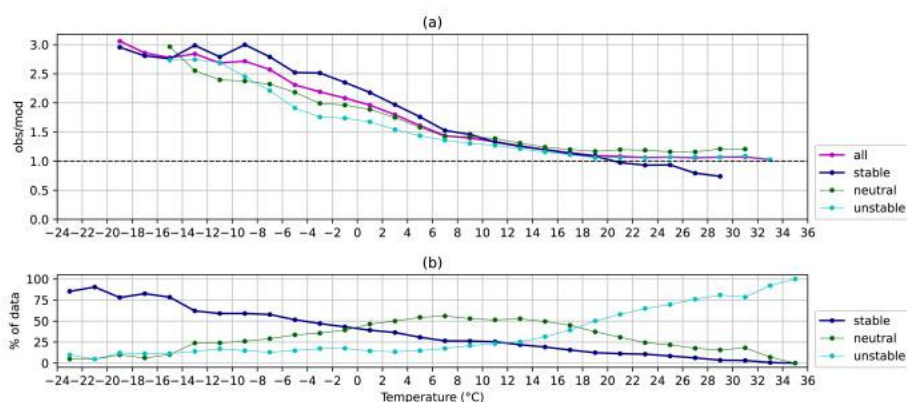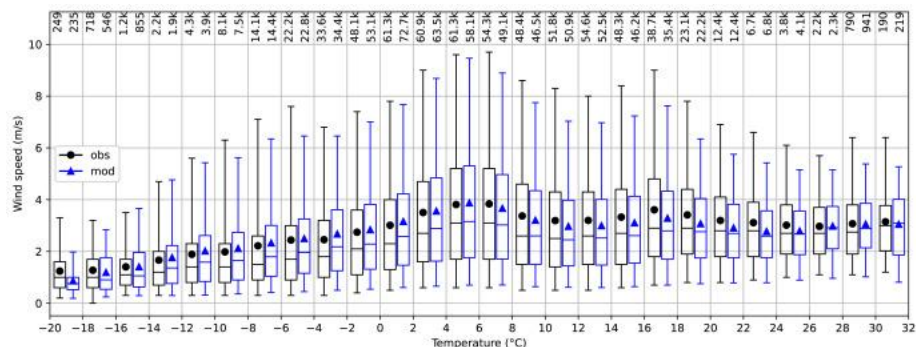

Download : Download high-res image (559KB)

Download : Download full-size image

Fig. 6. Temperature dependence of NO_x bias in different static stability regimes: The modelled Obukhov length L is used to categorise the data into stable (0m<L<200m), neutral (|L|>200m) and unstable (-200m<L<0m) regime. (a) The ratio of mean observed and modelled NO_x concentration in each 2°C temperature bin, for all data and for data in each stability regime. Only bins with at least 100 data values are plotted. (b) Distribution of data between the three stability regimes at each temperature.

In addition to vertical mixing, the 10-m wind speed is one of the most important variables for dilution and it has good observations at synoptic stations. To analyse the possibility that dilution is too high in the model at the low temperatures due to bias in wind speed, we therefore compared the observed and modelled wind speed as function of temperature. We selected synoptic stations closer than 10km to the NO_x stations. Of the 46 NO_x stations, 40 are closer than 10km to at least one synoptic station which measures both 10-m wind speed and 2-m temperature at hourly resolution. We picked the closest one of these in each case. This resulted in only 19 synoptic stations, since usually the NO_x stations in the same city all have the same closest synoptic station.

Fig. 7 shows the relationship between wind speed and temperature in the observations, and for the corresponding modelled values. It is clear from the figure that there is little systematic bias in wind speed at low temperature. So a dilution explanation to the NO_x bias is not apparent.

Download : Download high-res image (560KB)

Download : Download full-size image

Fig. 7. Distribution of hourly data of 10-m wind speed at different 2-m temperatures in 2016–2019at 19 synoptic stations in Norway located close to the NO_x monitoring stations: For each 2°C bin of observed/modelled temperature, the box plot to the left/right show the mean (circle/triangle), median (horizontal line), inter-quartile range (box) and 5–95% percentile range (whiskers) of observed/modelled wind speed. The number above each box plot indicates the number of hourly data values in the bin. The bins below -20°C and above +32°C are not shown because there are not at least 100 data values in both model and observations.

To further investigate a dilution bias as an explanation, we also plot the temperature dependence of the $PM_{2.5-10}$ concentration (Fig. 8). Compared to the corresponding figure for NO_x (Fig. 2), the model is close to the observations on average for all temperatures below 10°C. At high temperatures, the $PM_{2.5-10}$ is underestimated. At low temperatures, road traffic is the dominating local source of $PM_{2.5-10}$, just as for NO_x, but through the non-exhaust emissions. We would therefore expect to see a similar underestimation of $PM_{2.5-10}$at low temperatures as we see for NO_x if dilution were the main reason for the underestimation. Although the observed-to-modelled ratio of $PM_{2.5-10}$ concentration increases slightly with decreasing temperature from +4°C to -18°C, which might be an effect of dilution bias in cold conditions, this temperature dependence is much smaller than the one found for NO_x.
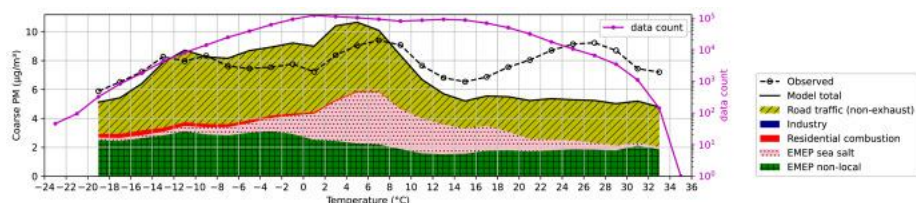
Download : Download high-res image (714KB)

Download : Download full-size image

Fig. 8. Same as Fig. 2a and c, but for the $PM_{2.5-10}$ concentration.

Though part of the NO_x temperature dependence can be caused by poor model representation of situations with stable conditions, the comparison with $PM_{2.5-10}$ shows that this effect is likely to be significantly smaller than the observed temperature dependence for NO_x concentrations.

4.5. Temperature correction

Assuming that the temperature dependence in observed-to-modelled ratio of NO_x found in section 4.2 is due to higher road traffic emissions at low temperatures, we can derive a temperature-dependent correction factor to be applied to the road traffic emissions. Since not all the NO_x comes from road traffic, we first need to isolate the road traffic contributions. Based on the analysis of contributions to the "EMEP non-local" (see section 4.1.1), we estimate that about 20% of the non-local comes from road traffic in Norway. The temperature-dependent bias is attributed to this part of the non-local as well as to the local road traffic contribution, which together comprise 82% of the total NO_x concentration in average. The remaining 80% of the non-local is assumed to have no temperature-dependent bias. We also neglect any road traffic contribution to the small negative bias that can be seen at high temperatures in Fig. 2a. From these assumptions, we can calculate the observed (O_{tra}) and modelled (M_{tra}) total road traffic contributions to NO_x in each temperature interval in Fig. 2:

$$M_{tra} = M_{tra,local} + f_{tra,nl} M_{nl} \tag{2}$$

$$O_{tra} = O_{tot} - (M_{tot} - M_{tra} - \varepsilon_{warm}) \tag{3}$$

where O_{tot} and M_{tot} are the total observed and modelled NO_x concentrations, respectively, $M_{tra,local}$ and M_{nl} are the modelled local road traffic and EMEP non-local contributions, respectively (shaded in Fig. 2), $f_{tra,nl}$=0.2, and ε_{warm}=−4.25 µg/m³ is the mean bias at temperatures above 14°C.

Fig. 9 shows O_{tra} and M_{tra} plotted in each temperature interval, and the ratio between them, for the same dataset as in Fig. 2. We use the same curve fitting approach that was applied to the total NO_x concentration in section 4.2 to create a function $f(T)$ (Equation (1)), but imposing f_1=1. The fit gives coefficient values f_0=3.28, T_0=-12.9°C, and T_1=12.4°C. The fit is plotted in Fig. 9b. Road traffic NO_x emissions can be multiplied by $f(T)$, using these coefficient values, in order to correct for the temperature dependence.
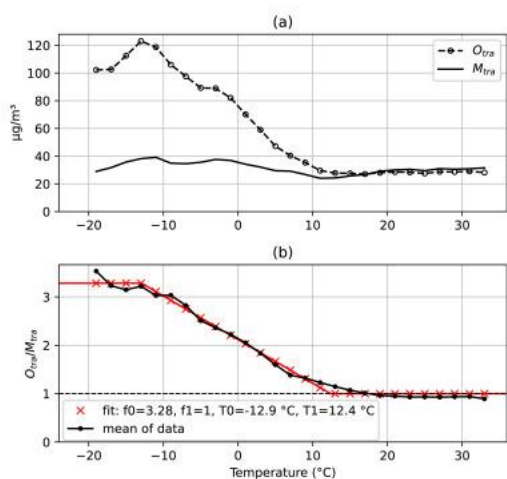
Download : Download high-res image (309KB)
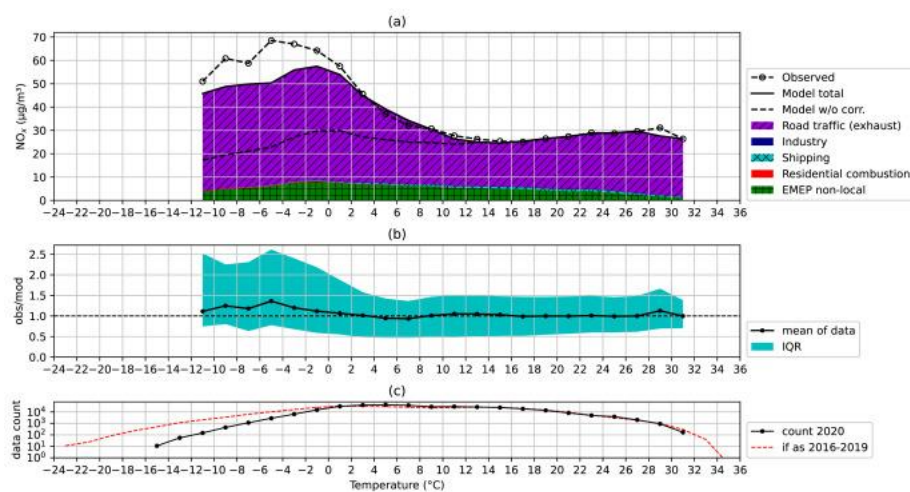
Download : Download full-size image

Fig. 9. As Fig. 2a and b, but plotting only the estimated road traffic contributions to NO_x (O_{tra} and M_{tra}, defined in section 4.5) instead of the total observed and modelled concentrations.

The correction implies that road traffic emissions are 2.7 times higher at -7°C than at the highest temperatures. However, this correction is applied to the emissions from the vehicle fleet as a whole, while we know that not all vehicles have important temperature dependence. If we use the approximation from section 2.3 that 82% of road traffic emissions in warm conditions come from the vehicles with temperature dependence, then the increase in emissions at -7°C for these vehicles must be a factor 3.1 in order to produce the same effect. This increase is within the range of 2–4 estimated in section 2.3.

4.6. Application to 2020

We performed a model run for the year 2020 applying the correction defined in section 4.5. This run also used updated road traffic emission factors for 2020 which account for geographic variation of the vehicle fleet, and it used traffic volume measurements (see section 3.3.1) to account for reduced road traffic during Covid-19 lockdown (mainly affecting March, April and May).

Fig. 10 shows the temperature dependence in the model run for 2020 compared to the observations. The correction removes the bias very well in the temperature range 2–14°C, while some bias still remains at temperatures below 2°C.

Fig. 10. Same as Fig. 2, but for a rerun of the year 2020, comparing to the available observations in this year. The correction described in section 4.5 has been applied to the NO_x road traffic emission input to the model. The dashed line in (a) is an estimate of the NO_x concentrations the model would give without this correction. In (c), the solid line is the actual data count in 2020, while the dashed line indicates what the data count would have been if the distribution of temperatures were the same in 2020 as in 2016–2019.

The winter months of 2020 were warmer than normal. There is therefore much less data in the range from -10 to 0°C than for the years 2016–2019 (Fig. 10c), and a small number of stations contributes to a large part of these data. We find that observed NO_x concentrations are higher in the model in 2020 than the other years at some of these stations without this being captured by the model (not shown). It is therefore likely that the remaining bias at low temperatures in 2020 is due to meteorological conditions around these stations that are not captured by the model. Nevertheless, the temperature correction still improves the performance significantly. Importantly the overall mean bias is just -2.4% in the 2020 rerun, compared to -29.0% when the correction is not included (dashed line in Fig. 10a).

5. Conclusion

The magnitude of temperature dependence of NO_x emissions from road traffic has been estimated in this study by comparing observed NO_x concentrations to modelled NO_x concentrations over a 4-year period at 46 Norwegian monitoring stations where NO_x sources are mostly road traffic.

We found a gradual increase in the average observed-to-modelled ratio of NO_x concentration with decreasing temperature, from 1.09 above +14.0°C to 2.90 below -13.4°C. Both below and above this range the ratio is approximately constant with temperature. This temperature dependence is quite similar between stations, seasons and years. Assuming it is due to the temperature dependence in road traffic emissions, a correction formula for these emissions was derived. The correction factor is 1 at high temperatures and 3.28 at low temperatures, with a linear increase in the range from +12.4°C to -12.9°C. This implies that road traffic emissions are 2.7 times higher at -7°C than in warm conditions. If we assume that the temperature effect mainly comes from diesel vehicles of Euro 4/IV or newer, then the emissions from these must be about 3.1 times higher at -7°C than in warm conditions. This increase is within the expected range of 2–4 based on the experimental studies of temperature dependence of diesel vehicles (section 2.3). Our results also indicate that the emissions continue to increase with decreasing temperature below -7°C.

In contrast to the NO_x concentrations, no temperature-dependent bias was found for the $PM_{2.5-10}$ concentrations, even though their local sources are also mostly from road traffic. We also did not find any systematic bias in the wind speed at low temperatures, and the analysis of different stability regimes (stable, neutral and unstable) showed that the temperature-dependent bias occurs in all three regimes. It is therefore more likely that the overall temperature-dependent bias in modelled NO_x concentrations in our dataset is due to emission bias than to bias in atmospheric transport. At some single stations or in shorter periods, bias in dilution or wind direction is probably important as well.

Since the correction is derived empirically, it might not be directly transferable to other time periods or areas, but if the vehicle fleet is similar it is likely to be a good approximation. However, the fleet changes over time. Battery electric vehicles and plug-in hybrids (PHEVs) make up a large fraction of new PCs in Norway (Manthey, 2021), and there is also an increase in battery electric urban buses. As a consequence, the relative HDV contribution to total NO_x emissions will increase. PHEVs' fraction of kilometres driven will increase as well, and uncertainty is related to the emissions from these as it largely depends on charging habits and driving mode (Figenbaum and Weber, 2016; Suarez-Bertoa et al., 2019). Hence, it is expected that this will influence the correction factor needed. Such future changes in the temperature dependence on

the road traffic emissions can be included by doing an update of the correction using the approach of section 4.2 with new years. However, overall fleet changes are relatively slow and average vehicle age for a PC is just below 11 years in Norway. We therefore expect the correction factor found also to be representative for several years. This is further supported by the similarity of the temperature dependence over the four years of observations used (Fig. 3).

We conclude that the NO_x emissions from road traffic can be corrected for the temperature dependence by using the method presented in this article, and the derived temperature correction will be applied in future modelling of NO_x pollution in Norway.

CRediT authorship contribution statement

Eivind G. Wærsted: Investigation, Formal analysis, Visualization, Writing – original draft. **Ingrid Sundvor:** Conceptualization, Writing – original draft, Writing – review & editing. **Bruce R. Denby:** Conceptualization, Methodology, Supervision, Writing – review & editing. **Qing Mu:** Formal analysis.

Declaration of competing interest

The authors declare that they have no known competing financial interests or personal relationships that could have appeared to influence the work reported in this paper.

Acknowledgements

Recommended articles

References

Bernard et al., 2019   Y. Bernard, J. German, A. Kentroti, R. Muncrief
Catching defeat devices: how systematic vehicle testing can determine the presence of suspicious emissions control strategies
Tech. Rep.Int. Counc. Clean.Transport (2019)
URL:
https://theicct.org/publications/detecting-defeat-devices-201906 ↗
Google Scholar ↗

Copat et al., 2020   C. Copat, A. Cristaldi, M. Fiore, A. Grasso, P. Zuccarello, S. Santo Signorelli, G.O. Conti, M. Ferrante
The role of air pollution (PM and NO2) in COVID-19 spread and lethality: a systematic review
Environ. Res., 191 (2020), 10.1016/j.envres.2020.110129 ↗
Google Scholar ↗

Dardiotos et al., 2012   C. Dardiotos, G. Martini, A. Marotta, U. Manfredi
Extension of Low Temperature Emission Test to Euro 6 Diesel Vehicles. Report EUR 25408
European Union – Joint Research Centre (2012), 10.2788/37683 ↗
Google Scholar ↗

Dardiotos et al., 2013   C. Dardiotos, G. Martini, A. Marotta, U. Manfredi
Low-temperature cold-start gaseous emissions of late technology passenger cars
Appl. Energy, 111 (2013), pp. 468-478, 10.1016/j.apenergy.2013.04.093 ↗
Google Scholar ↗

Denby, 2011   B. Denby
Source apportionment of PM2.5 in urban areas using multiple linear regression as an inverse modelling technique
Int. J. Environ. Pollut., 47 (2011), pp. 60-69, 10.1504/IJEP.2011.047326 ↗
View in Scopus ↗   Google Scholar ↗

Denby et al., 2020   B.R. Denby, M. Gauss, P. Wind, Q. Mu, E.G. Wærsted, H. Fagerli, A. Valdebenito, H. Klein
Description of the uEMEP_v5 downscaling approach for the EMEP MSC-W chemistry transport model
Geosci. Model Dev. (GMD), 13 (2020), pp. 6303-6323, 10.5194/gmd-13-6303-2020 ↗

Google Scholar ↗

Denby et al., 2018 B.R. Denby, K.J. Kupiainen, M. Gustafsson

Review of road dust emissions

F. Amato (Ed.), Non-Exhaust Emissions: an Urban Air Quality Problem for Public Health; Impact and Mitigation Measures, Academic Press, San Diego (2018), pp. 183-203, 10.1016/B978-0-12-811770-5.00009-1 ↗

(chapter 9)

📄 View PDF   View article   View in Scopus ↗   Google Scholar ↗

Denby et al., 2013a B.R. Denby, I. Sundvor, C. Johansson, L. Pirjola, M. Ketzel, M. Norman, K. Kupiainen, M. Gustafsson, G. Blomqvist, M. Kauhaniemi, G. Omstedt

A coupled road dust and surface moisture model to predict non-exhaust road traffic induced particle emissions (NORTRIP). Part 2: surface moisture and salt impact modelling

Atmos. Environ., 81 (2013), pp. 485-503, 10.1016/j.atmosenv.2013.09.003 ↗

📄 View PDF   View article   View in Scopus ↗   Google Scholar ↗

Denby et al., 2013b B.R. Denby, I. Sundvor, C. Johansson, L. Pirjola, M. Ketzel, M. Norman, K. Kupiainen, M. Gustafsson, G. Blomqvist, G. Omstedt

A coupled road dust and surface moisture model to predict non-exhaust road traffic induced particle emissions (NORTRIP). Part 1: road dust loading and suspension modelling

Atmos. Environ., 77 (2013), pp. 283-300, 10.1016/j.atmosenv.2013.04.069 ↗

📄 View PDF   View article   View in Scopus ↗   Google Scholar ↗

Directive 2008/50EC, 2008 Directive 2008/50EC

Directive 2008/50/EC of the European Parliament and of the Council of 21 May 2008 on Ambient Air Quality and Cleaner Air for Europe

(2008)

URL:

https://eur-lex.europa.eu/legal-content/en/ALL/?uri=CELEX:32008L0050 ↗

Google Scholar ↗

Directive 98/69/EC, 1998 Directive 98/69/EC

Directive 98/69/EC of the European Parliament and of the Council of 13 October 1998 relating to measures to be taken against air pollution by emissions from motor vehicles and amending Council Directive 70/220/EEC

URL:

https://eur-lex.europa.eu/legal-content/en/ALL/?uri=CELEX%3A31998L0069 ↗ (1998)

Google Scholar ↗

ECMWF, 2020 ECMWF

IFS: documentation of the integrated forecasting system

URL:

https://www.ecmwf.int/en/publications/ifs-documentation ↗ (2020)

Google Scholar ↗

European Commission, 2021 European Commission

Emissions in the automotive sector

URL:

https://ec.europa.eu/growth/sectors/automotive/environment-protection/emissions_en ↗ (2021)

Google Scholar ↗

European Environment Agency, 2020 European Environment Agency

Air quality in Europe - 2020 report

EEA Report, 9 (2020), 10.2800/786656 ↗

European Environment Agency

Google Scholar ↗

European Union, 2016 European Union

Replies from car manufacturers to EMIS questionnaire

URL:
https://www.europarl.europa.eu/committees/en/archives/8/emis/home/publications?tabCode=evidence ↗ (2016)

Google Scholar ↗

Faria et al., 2018   M.V. Faria, R.A. Varella, G.O. Duarte, T.L. Farias, P.C. Baptista

Engine cold start analysis using naturalistic driving data: city level impacts on local pollutants and energy consumption

Sci. Total Environ., 630 (2018), pp. 544-559, 10.1016/j.scitotenv.2018.02.232 ↗

🔲 View PDF   View article   View in Scopus ↗   Google Scholar ↗

Figenbaum and Weber, 2016   E. Figenbaum, C. Weber

Experimental testing of Plug-in Hybrid vehicles; CO2-emission, energy consumption and local pollution. Report 1539/2016. Institute of Transport Economics (TØI)

URL:
https://www.toi.no/publications/experimental-testing-of-plug-in-hybrid-vehicles-co2-emission-energy-consumption-and-local-pollution-article34298-29.html ↗ (2016)

Google Scholar ↗

Grange et al., 2019   S.K. Grange, N.J. Farren, A.R. Vaughan, R.A. Rose, D.C. Carslaw

Strong temperature dependence for light-duty diesel vehicle NO_x emissions

Environ. Sci. Technol., 53 (2019), pp. 6587-6596, 10.1021/acs.est.9b01024 ↗

View in Scopus ↗   Google Scholar ↗

Granier et al., 2019   C. Granier, S. Darras, H. Denier van der Gon, J. Doubalova, N. Elguindi, B. Galle, M. Gauss, M. Guevara, J.P. Jalkanen, J. Kuenen, C. Liousse, B. Quack, D. Simpson, K. Sindelarova

The Copernicus Atmosphere Monitoring Service Global and Regional Emissions (April 2019 Version). ECMWF Copernicus Report

Copernicus Atmosphere Monitoring Service (2019), 10.24380/d0bn-kx16 ↗

Google Scholar ↗

Grigoratos et al., 2019   T. Grigoratos, G. Fontaras, B. Giechaskiel, N. Zacharof

Real world emissions performance of heavy-duty Euro VI diesel vehicles

Atmos. Environ., 201 (2019), pp. 348-359, 10.1016/j.atmosenv.2018.12.042 ↗

🔲 View PDF   View article   View in Scopus ↗   Google Scholar ↗

Gryning et al., 1987   S.E. Gryning, A.A.M. Holtslag, J.S. Irwin, B. Sivertsen

Applied dispersion modelling based on meteorological scaling parameters

Atmos. Environ., 1967 (21) (1987), pp. 79-89, 10.1016/0004-6981(87)90273-3 ↗

🔲 View PDF   View article   View in Scopus ↗   Google Scholar ↗

Grythe et al., 2019   H. Grythe, S. Lopez-Aparicio, M. Vogt, D. Vo Thanh, C. Hak, A.K. Halse, P. Hamer, G. Sousa Santos

The MetVed model: development and evaluation of emissions from residential wood combustion at high spatio-temporal resolution in Norway

Atmos. Chem. Phys., 19 (2019), pp. 10217-10237, 10.5194/acp-19-10217-2019 ↗

View in Scopus ↗   Google Scholar ↗

Hausberger and Matzer, 2017   S. Hausberger, C. Matzer

Update of Emission Factors for Euro 3, Euro 5 and Euro 6 Diesel Passenger Cars for the HBEFA Version 3.3. Technical Report I-09/17 CM EM 16/26/679

Graz University of Technology (2017)

URL:
https://www.hbefa.net/e/documents/HBEFA3-3_TUG_finalreport_01062016.pdf ↗

Google Scholar ↗

Hausberger et al., 2009   S. Hausberger, M. Rexeis, M. Zallinger, R. Luz

Emission Factors from the Model PHEM of the HBEFA Version 3. Technical Report I-20/2009 Haus-Em 33/08/679

Graz University of Technology (2009)

URL:

https://www.hbefa.net/e/documents/HBEFA_31_Docu_hot_emissionfactors_PC_LCV_HDV.pdf ↗

Google Scholar ↗

Holmengen and Fedoryshyn, 2015   N. Holmengen, N. Fedoryshyn

Utslipp fra veitrafikken i Norge. Dokumentasjon av beregningsmetoder, data og resultater. Notater 2015/22. Statistics Norway

URL:

https://www.ssb.no/natur-og-miljo/artikler-og-publikasjoner/utslipp-fra-veitrafikken-i-norge ↗ (2015)

Google Scholar ↗

Hooftman and de Ruiter, 2019   N. Hooftman, J. de Ruiter

Tampering. Report D1.3. uCARe consortium, TNO, den haag

URL:

http://resolver.tudelft.nl/uuid:60f925d8-a3ca-49a4-840e-a93dc2b10233 ↗ (2019)

Google Scholar ↗

Hovi et al., 2019   I.B. Hovi, D.R. Pinchasik, R.J. Thorne, E. Figenbaum

User Experiences from the Early Adopters of Heavy-Duty Zero-Emission Vehicles in Norway. Barriers and Opportunities. TØI Report 1734/2019

Institute of Transport Economics (2019)

URL:

https://www.toi.no/publikasjoner/erfaringer-fra-tidlige-brukere-av-nullutslippslosninger-for-tunge-kjoretoy-i-norge-article35935-8.html ↗

Google Scholar ↗

Huangfu and Atkinson, 2020   P. Huangfu, R. Atkinson

Long-term exposure to NO2 and O3 and all-cause and respiratory mortality: a systematic review and meta-analysis

Environ. Int., 144 (2020), 10.1016/j.envint.2020.105998 ↗

Google Scholar ↗

Ko et al., 2017   J. Ko, D. Jin, W. Jang, C.L. Myung, S. Kwon, S. Park

Comparative investigation of NO_x emission characteristics from a Euro 6-compliant diesel passenger car over the NEDC and WLTC at various ambient temperatures

Appl. Energy, 187 (2017), pp. 652-662, 10.1016/j.apenergy.2016.11.105 ↗

🔴 View PDF   View article   View in Scopus ↗   Google Scholar ↗

Kuenen et al., 2014   J.J.P. Kuenen, A.J.H. Visschedijk, M. Jozwicka, H.A.C. Denier Van Der Gon

TNO-MACC_II emission inventory; a multi-year (2003–2009) consistent high-resolution European emission inventory for air quality modelling

Atmos. Chem. Phys., 14 (2014), pp. 10963-10976, 10.5194/acp-14-10963-2014 ↗

View in Scopus ↗   Google Scholar ↗

Kuik et al., 2018   F. Kuik, A. Kerschbaumer, A. Lauer, A. Lupascu, E. von Schneidemesser, T.M. Butler

Top–down quantification of NO_x emissions from traffic in an urban area using a high-resolution regional atmospheric chemistry model

Atmos. Chem. Phys., 18 (2018), pp. 8203-8225, 10.5194/acp-18-8203-2018 ↗

View in Scopus ↗   Google Scholar ↗

Lapuerta et al., 2018   M. Lapuerta, A. Ramos, J. Barba, D. Fernandez-Rodriguez

Cold- and warm-temperature emissions assessment of n-butanol blends in a Euro 6 vehicle

Appl. Energy, 218 (2018), pp. 173-183, 10.1016/j.apenergy.2018.02.178 ↗

🔴 View PDF   View article   View in Scopus ↗   Google Scholar ↗

Lussana et al., 2019   C. Lussana, I.A. Seierstad, T.N. Nipen, L. Cantarello

Spatial interpolation of two-metre temperature over Norway based on the combination of numerical weather prediction ensembles and in situ observations

Q. J. R. Meteorol. Soc., 145 (2019), pp. 3626-3643, 10.1002/qj.3646 ↗

View in Scopus ↗   Google Scholar ↗

Manthey, 2021 N. Manthey

Norway Registers 84.8% Market Share of Plug-In Cars in March

electrive.com (2021)

URL:

https://www.electrive.com/2021/04/07/norway-registers-84-8-marketshare-of-plug-in-cars-in-march/ ↗

Google Scholar ↗

Matzer et al., 2019 C. Matzer, K. Weller, M. Dippold, S. Lipp, M. Röck, M. Rexeis, S. Hausberger

Update of Emission Factors for HBEFA Version 4.1; Final Report. Technical Report I-05/19/CM EM-I-16/26/679

Graz University of Technology (2019)

URL:

https://www.hbefa.net/e/documents/HBEFA41_Report_TUG_09092019.pdf ↗

Google Scholar ↗

McCaffery et al., 2021 C. McCaffery, H. Zhu, T. Tang, C. Li, G. Karavalakis, S. Cao, A. Oshinuga, A. Burnette, K.C. Johnson, T.D. Durbin

Real-world NO_x emissions from heavy-duty diesel, natural gas, and diesel hybrid electric vehicles of different vocations in California roadways

Sci. Total Environ., 784 (2021), 10.1016/j.scitotenv.2021.147224 ↗

Google Scholar ↗

Müller et al., 2017 M. Müller, M. Homleid, K.I. Ivarsson, M.A.Ø. Køltzow, M. Lindskog, K.H. Midtbø, U. Andrae, T. Aspelien, L. Berggren, D. Bjørge, P. Dahlgren, J. Kristiansen, R. Randriamampianina, M. Ridal, O. Vignes

AROME-MetCoOp: a Nordic convective-scale operational weather prediction model

Weather Forecast., 32 (2017), pp. 609-627, 10.1175/WAF-D-16-0099.1 ↗

View in Scopus ↗   Google Scholar ↗

Nipen et al., 2020 T.N. Nipen, I.A. Seierstad, C. Lussana, J. Kristiansen, Ø. Hov

Adopting citizen observations in operational weather prediction

Bull. Am. Meteorol. Soc., 101 (2020), pp. E43-E57, 10.1175/BAMS-D-18-0237.1 ↗

View in Scopus ↗   Google Scholar ↗

Nordbeck and Langsrud, 2015 O. Nordbeck, Ø. Langsrud

Modellering av trafikk på kommunale veier. Beskrivelse av metode. Notater 2015/46. Statistics Norway

URL:

https://www.ssb.no/transport-og-reiseliv/artikler-og-publikasjoner/modellering-av-trafikk-pa-kommunale-veier ↗ (2015)

Google Scholar ↗

Norwegian Environment Agency, 2014 Norwegian Environment Agency

Håndbok for Kvalitetssystem for Målinger Av Luftkvalitet. Veileder (Guidance Document) M39-2014

Norwegian Environment Agency (2014)

URL:

https://www.miljodirektoratet.no/publikasjoner/2014/januar-2014/handbok-for-kvalitetssystem-for-malinger-av-luftkvalitet/ ↗

Google Scholar ↗

NVDB, 2020 NVDB

Nasjonal vegdatabank, Statens Vegvesen (Norwegian national road database)

URL:

https://www.vegvesen.no/fag/teknologi/nasjonal+vegdatabank ↗ (2020)

Google Scholar ↗

Orellano et al., 2020 P. Orellano, J. Reynoso, N. Quaranta, A. Bardach, A. Ciapponi

Short-term exposure to particulate matter (PM10 and PM2.5), nitrogen dioxide (NO2), and ozone (O3) and all-cause and cause-specific mortality: systematic review and meta-analysis

Environ. Int., 142 (2020), 10.1016/j.envint.2020.105876 ↗

Google Scholar ↗

Söderena et al., 2021 P. Söderena, H. Kuutti, A.P. Pellikka

Euro VI diesel city buses NOx emissions monitoring. VTT research report VTT-R-00567-21. VTT technical research Centre of Finland

URL:

https://cris.vtt.fi/en/publications/euro-vi-diesel-city-buses-nox-emissions-monitoring ↗ (2021)

Google Scholar ↗

Söderena et al., 2020   P. Söderena, J. Laurikko, C. Weber, A. Tilli, K. Kuikka, A. Kousa, O. Väkevä, A. Venho, S. Haaparanta, J. Nuottimäki

Monitoring Euro 6 diesel passenger cars NOx emissions for one year in various ambient conditions with PEMS and NOx sensors

Sci. Total Environ., 746 (2020), 10.1016/j.scitotenv.2020.140971 ↗

Google Scholar ↗

Simpson et al., 2012   D. Simpson, A. Benedictow, H. Berge, R. Bergström, L.D. Emberson, H. Fagerli, C.R. Flechard, G.D. Hayman, M. Gauss, J.E. Jonson, M.E. Jenkin, A. Nyíri, C. Richter, V.S. Semeena, S. Tsyro, J.P. Tuovinen, Á. Valdebenito, P. Wind

The EMEP MSC-W chemical transport model – technical description

Atmos. Chem. Phys., 12 (2012), pp. 7825-7865, 10.5194/acp-12-7825-2012 ↗

View in Scopus ↗   Google Scholar ↗

Statistics Norway, 2020   Statistics Norway

08941: acidification precursors, ozone precursors etc., by source, energy product and pollutant

URL:

https://www.ssb.no/en/statbank/table/08941/ ↗ (2020)

Google Scholar ↗

Suarez-Bertoa and Astorga, 2018   R. Suarez-Bertoa, C. Astorga

Impact of cold temperature on Euro 6 passenger car emissions

Environ. Pollut., 234 (2018), pp. 318-329, 10.1016/j.envpol.2017.10.096 ↗

🗎 View PDF   View article   View in Scopus ↗   Google Scholar ↗

Suarez-Bertoa et al., 2019   R. Suarez-Bertoa, J. Pavlovic, G. Trentadue, M. Otura-Garcia, A. Tansini, B. Ciuffo, C. Astorga

Effect of low ambient temperature on emissions and electric range of plug-in hybrid electric vehicles

ACS Omega, 4 (2019), pp. 3159-3168, 10.1021/acsomega.8b02459 ↗

View in Scopus ↗   Google Scholar ↗

Thorne et al., 2021   R.J. Thorne, I.B. Hovi, E. Figenbaum, D.R. Pinchasik, A.H. Amundsen, R. Hagman

Facilitating adoption of electric buses through policy: learnings from a trial in Norway

Energy Pol., 155 (2021), 10.1016/j.enpol.2021.112310 ↗

Google Scholar ↗

Tu et al., 2021   R. Tu, J. Xu, A. Wang, Z. Zhai, M. Hatzopoulou

Effect of ambient temperature and cold starts on excess NO_X emissions in a gasoline direct injection vehicle

Sci. Total Environ., 760 (2021), 10.1016/j.scitotenv.2020.143402 ↗

Google Scholar ↗

Wang et al., 2018   J.M. Wang, C.H. Jeong, N. Zimmerman, R.M. Healy, G.J. Evans

Real world vehicle fleet emission factors: seasonal and diurnal variations in traffic related air pollutants

Atmospheric Environement, 184 (2018), pp. 77-86, 10.1016/j.atmosenv.2018.04.015 ↗

🗎 View PDF   View article   Google Scholar ↗

Weber et al., 2019   C. Weber, I. Sundvor, E. Figenbaum

Comparison of regulated emission factors of Euro 6 LDV in Nordic temperatures and cold start conditions: diesel- and gasoline direct-injection

Atmospheric Environement, 206 (2019), pp. 208-216, 10.1016/j.atmosenv.2019.02.031 ↗

Google Scholar ↗

Weilenmann et al., 2009   M. Weilenmann, J.Y. Favez, R. Alvarez

Cold-start emissions of modern passenger cars at different low ambient temperatures and their evolution over vehicle legislation categories

Atmospheric Environement, 43 (2009), pp. 2419-2429, 10.1016/j.atmosenv.2009.02.005 ↗

📄 View PDF   View article   View in Scopus ↗   Google Scholar ↗

World Health Organization, 2013   World Health Organization

Review of Evidence on Health Aspects of Air Pollution – REVIHAAP Project: Final Technical Report

Technical report. World Health Organization (2013)

URL:

https://www.euro.who.int/en/health-topics/environment-and-health/air-quality/publications/2013/review-of-evidence-on-health-aspects-of-air-pollution-revihaap-project-final-technical-report ↗

Google Scholar ↗

Zheng et al., 2021   X.Y. Zheng, P. Orellano, H.L. Lin, M. Jiang, W.J. Guan

Short-term exposure to ozone, nitrogen dioxide, and sulphur dioxide and emergency department visits and hospital admissions due to asthma: a systematic review and meta-analysis

Environ. Int., 150 (2021), 10.1016/j.envint.2021.106435 ↗

Google Scholar ↗

Cited by (3)

The importance of data splitting in combined NO$_x$ concentration modelling

2023, Science of the Total Environment

Show abstract ∨

Analysis of Seasonal Variation and Dispersion Pattern of Ambient Air Pollutants in an Urban Environment

2022, ResearchSquare

Decoupling Emission Reductions and Trade-Offs of Policies in Norway Based on a Bottom-Up Traffic Emission Model

2022, Atmosphere

1   Table 3 indicates the share of long vehicles and not HDV, since the automatic counting data discriminate on length and not weight (see section 3.3.1). However, the variability between stations is assumed to be similar for HDV share.

2   GNFR = Gridded Nomenclature For Reporting, see Granier et al. (2019).